# Theoretical Investigation of the Low-Energy States of $CpMoCl(PMe_3)_2$ and Their Role in the Spin-Forbidden Addition of $N_2$ and CO

**Vidar R. Jensen*,† and Rinaldo Poli*,‡**

*Laboratoire de Synthèse et d'Electrosynthèse Organométalliques, Faculté des Sciences "Gabriel", Université de Bourgogne, 6 Boulevard Gabriel, F-21000, Dijon, France*

*Received: October 15, 2002; In Final Form: December 23, 2002*

A recent computational investigation of Jahn−Teller effects in unsaturated 16-electron $d^4$—$d^6$ [$CpML_n$] complexes (Abu-Hasanayn, F.; Cheong, P.; Oliff, M. *Angew. Chem.* **2002**, *41*, 2120) highlighted the typical presence of two spin-triplet and two singlet states of competing stability in these complexes and pointed out the necessity to account for more than one electronic state in studies thereof. Consequently, we have reinvestigated the addition of $N_2$ to all the four low-energy states of $CpMoCl(PH_3)_2$, a reaction for which previously only one singlet and one triplet state have been considered (Keogh, D. W.; Poli, R. *J. Am. Chem. Soc.* **1997**, *119*, 2516). The present study was performed using density functional theory (DFT) and the thus obtained relative stabilities of the four electronic states of the educt are in good accord with those obtained using a multireference MP2 method. The spin-singlet ground state of the $18e^-$ product of $N_2$ addition turns out to be derived from the fourth lowest state ($2^1A'$) of the $16e^-$ educt, immediately demonstrating the importance of accounting for more than one triplet and one singlet state in such reactions. The barrier to $N_2$ addition was found to arise from the enthalpic cost of obtaining identical geometries for this singlet state and the spin-triplet ground state of the educt ($^3A''$) in the minimum energy crossing point (MECP). With a spin-triplet ground-state reactant complex, a triplet−singlet MECP defining the rate-limiting step, and a singlet product, our calculated activation (14.4 kcal/mol) as well as reaction enthalpies (21.2 kcal/mol) of $N_2$ addition to $CpMoCl(PMe_3)_2$ are found to be within the experimental error bars of those measured for $Cp^*MoCl(PMe_3)_2$. For the corresponding reaction with CO, there is a delicate balance between the transition state (TS) of addition on the triplet potential energy surface (PES) and the point of crossing between the triplet and singlet PES. Our optimized TS and MECPs for this reaction suggest that the rate is controlled by the barrier defined by the spin-triplet TS, with spin inversion occurring after this point. Our calculated activation enthalpy (6.7 kcal/mol) based on the spin-triplet TS is in excellent agreement with that measured for $Cp^*MoCl(PMe_3)_2$.

## Introduction

Thermal reactions that involve more than one spin potential energy surface (PES) are becoming the topic of increasing interest.[1−4] These are either processes leading from reagents in a particular spin state to products in a different spin state, or processes involving an even number of spin-state changes along the reaction pathway, leading to products in the same spin state as the reagents. In the latter case, the point at which the spin change occurs (minimum-energy crossing point, or MECP) may be located at a lower energy than that of the transition states (TSs) on the diabatic PES of the reagents and products. When this happens, the reaction can be considered to benefit from a spin-acceleration phenomenon.[5]

This general area, also termed "multiple-state reactivity" or "spin-crossover reactivity", is quite distinct from the more widely appreciated field of photochemical reactivity since no photon-coupled excitation or decay processes are involved. It has been shown to be relevant in gas-phase reactions of highly unsaturated metal-containing fragments,[6−9] in biochemically relevant processes,[10−13] in C−H-activation processes by organometallic complexes,[14,15] and in olefin-polymerization catalysis.[16−20] Unsaturated organometallic complexes (e.g. with less than 18 electrons in the valence shell) may be energetically stabilized by the adoption of a ground state with two or more unpaired electrons and stable examples of this family of molecules now abound.[21] Spin-crossover reactions may therefore be more common than previously appreciated in organometallic chemistry.

A few years ago, one of us carried out experimental and theoretical investigations of the addition process of CO and $N_2$ to the 16-electron spin-triplet complex $Cp^*MoCl(PMe_3)_2$,[22] leading to the spin-singlet 18-electron adducts, $Cp^*MoCl(PMe_3)_2(L)$ (L = CO or $N_2$). The large difference between the rates (CO reacts ca. 3 orders of magnitude faster than $N_2$) is at odds with the essentially equivalent rate that was previously determined for several other 16-electron intermediates. The calculations, which were carried out at the MP2/LANL2DZ level on the $CpMoCl(PH_3)_2$ model, allowed an interpretation of the phenomenon on the basis of a greater spin-change related enthalpic barrier for the $N_2$-addition process. The calculations along the reaction coordinate of addition involved only the triplet surface that derives from the ground state of the educt and the singlet state surface that derives from the adduct. A recent theoretical study by Abu-Hasanayn et al.,[23] however, has pointed

† Present address: Department of Chemistry, University of Bergen, N-5007 Bergen, Norway. E-mail: vidar.jensen@kj.uib.no.
‡ E-mail: poli@u-bourgogne.fr.

10.1021/jp027212y CCC: $25.00 
Published on Web 02/07/2003

out the typical presence of more than one electronic configuration in each spin state for 16-electron fragments, leading to different states with similar energy. We have therefore decided to reinvestigate our system under this new light and report our findings in the following.

## Computational Details

All geometry optimizations were performed using the three-parameter hybrid density functional method of Becke (termed B3LYP),[24] as implemented in the Gaussian98 set of programs.[25] Stationary points were optimized and characterized using algorithms involving analytic calculation of the first and second derivatives of the energy. The PESs of $N_2$ and CO addition were explored using linear transit (LT) calculations, i.e., series of geometry optimizations using constrained (frozen) Mo−$N_2$ and Mo−CO distances. In addition, the LT optimizations for the $2^1A'$ state of $CpMoCl(PH_3)_2$ were performed with the angle Mo−N−N constrained to the value optimized for the addition product in order to avoid complexation of the second N atom. For $N_2$ addition to $CpMoCl(PH_3)_2$, these optimizations were performed within $C_s$ symmetry in order to distinguish between the different electronic states and the curvature of the PES was monitored by calculation of the Hessian matrix. The reported structures always involve the energetically lowest of the two possible rotational conformations of the cyclopentadienyl ligand in the $C_s$ symmetrical complexes. The unrestricted formulation was used for triplet states whereas singlet states were obtained within the restricted formulation in order to avoid spin contamination. Numerical integrations were performed using the "ultrafine" grid of Gaussian98, consisting of 99 radial shells and 590 angular points per shell, and the Gaussian98 default values were chosen for the self-consistent field (SCF) and geometry optimization convergence criteria. Thermochemical values were computed within the harmonic-oscillator, rigid-rotor, and ideal-gas approximations. MECPs were located using the method described by Harvey et al.,[26] whereas the corresponding frequencies were calculated from an effective Hessian matrix.[26,27]

The B3LYP-optimized geometries were subjected to single-point (SP) energy calculations where indicated. In addition to the already described B3LYP method, SP calculations were performed using the BPW91 functional which contains the local exchange-correlation potential developed by Vosko et al.[28] augmented with Becke's[29] nonlocal exchange corrections and Perdew and Wang's[30] nonlocal correlation corrections. The SP calculations based on density functional theory (DFT) were performed using the "ultrafine" grid described above and the SCF procedure was converged to a RMS change of the density matrix below $1.0 \times 10^{-6}$. For the 16-electon educts, $CpMoCl(PH_3)_2$, SP energy calculations were also performed using a variant of multireference second-order perturbation theory, the MRMP2 method of Nakano[31,32] as implemented in the GAMESS-US set of programs.[33] This method gives results for the singlet−triplet splitting of methylene in close agreement with CASPT2. The reference wave functions were of the complete active space SCF type (CASSCF) and the active orbital space consisted of the three Mo 4d orbitals occupied in the triplet ground state, ($^3A''$, d-occupancy $(1a')^2(2a')^1(a'')^1$). Such a four-electron-three-orbital CASSCF model space was used throughout. All valence electrons were correlated in the subsequent perturbational calculations.

The basis sets that were used for the geometry optimizations (termed DZP) are described as follows: Hay and Wadt effective core potentials (ECP)[34,35] were used for the elements Mo, Cl, and P. For Mo, the ECP replaced the 1s, 2s, 2p, 3s, 3p, and 3d electrons whereas the 1s, 2s, and 2p electrons were replaced for the Cl and P atoms. The 4s, 4p, 4d, 5s, and 5p orbitals of Mo were described by the Hay and Wadt primitive basis set[35] contracted to [3s,3p,2d]. The 3s and 3p orbitals of Cl and P were described by Hay and Wadt primitive basis sets[34,35] augmented with a single diffuse p primitive[36] and a single polarization d primitive[36] and contracted to [2s,3p,1d]. Oxygen, nitrogen, carbon, and hydrogen atoms were described by standard Dunning and Hay valence double-$\zeta$ basis sets.[37] The basis sets of the atoms of the coordinating molecules (CO or $N_2$) were extended with a d polarization function.[36]

The SP energy calculations involved basis sets (termed TZD2P) that were improved compared to those used during the geometry optimizations: For molybdenum, the Hay and Wadt primitive basis was extended with three f primitives ($\alpha_f$ = 1.8913, 0.6783, and 0.2904) and contracted to [4s,4p,3d,2f]. For Cl and P atoms, the extended Hay and Wadt primitive basis set described above was contracted to [3s,4p,1d]. For carbon atoms forming part of the cyclopentadienyl ring, the standard valence double-$\zeta$ basis set was extended with a diffuse p primitive[36] and a single d polarization primitive[36] and contracted to [3s,-3p,1d]. For N, O, and C atoms of the coordinating molecule (CO or $N_2$) this [3s,3p,1d] basis set was extended in the following manner: A diffuse s function was added even-temperedly and a second uncontracted d function was added by splitting (with a factor = 3) the values of the single polarization function exponents, leading to [4s,3p,2d] contracted basis sets.

## Results and Discussion

**Addition of $N_2$ to $CpMoCl(PH_3)_2$.** Abu-Hasanayn et al.[23] recently pointed out the importance of accounting explicitly for two singlet and two triplet states in complexes such as $CpMo(CO)_2Cl$. Accordingly, one of the goals of the present study is to investigate the potential involvement of more than one electronic state of each spin (singlet and triplet) in reactions of $N_2$ and CO addition to $Cp^*MoCl(PMe_3)_2$. We thus decided to calculate the four energetically lowest lying potential curves of $N_2$ coordination to the computationally tractable $CpMoCl(PH_3)_2$ as shown in Figure 1. These linear transit (LT) calculations (series of optimizations with constrained Mo−N distances, see the Computational Details section) were performed under the assumption of $C_s$ symmetry in order to cleanly define the various electronic states on the basis of their differing total symmetry and/or orbital occupancy.

Starting with the educts, $CpMoCl(PH_3)_2$, vibrational analysis shows that the optimized $C_s$ symmetric geometries given in Figure 1 are true minima for the triplet ground state ($^3A''$, d-occupancy $(1a')^2(2a')^1(a'')^1$) as well as the second singlet state ($2^1A'$, $(1a')^2(a'')^2$). The lowest lying states of each spin multiplicity are also well-defined in $C_1$ symmetry. For the ground state, no lower lying point of $C_1$ symmetry could be found. Both $1^1A'$ ($(1a')^2(2a')^2$) and $^3A'$ ($(a'')^2(1a')^1(2a)^1$) are first-order saddle points. Relaxing the imposed symmetry restriction of the lowest lying singlet state results in only minor geometric changes and a negligible lowering of the energy (0.03 kcal/mol). The excited triplet state carries a residual imaginary frequency (132i $cm^{-1}$) corresponding to a relative rotation of the two $PH_3$ groups from eclipsed to staggered conformation, but this conformational issue presumably is of minor importance for the present addition reactions.

The geometrical parameters and relative energies for the educts are given in Table 1. The large difference in P−Mo−P

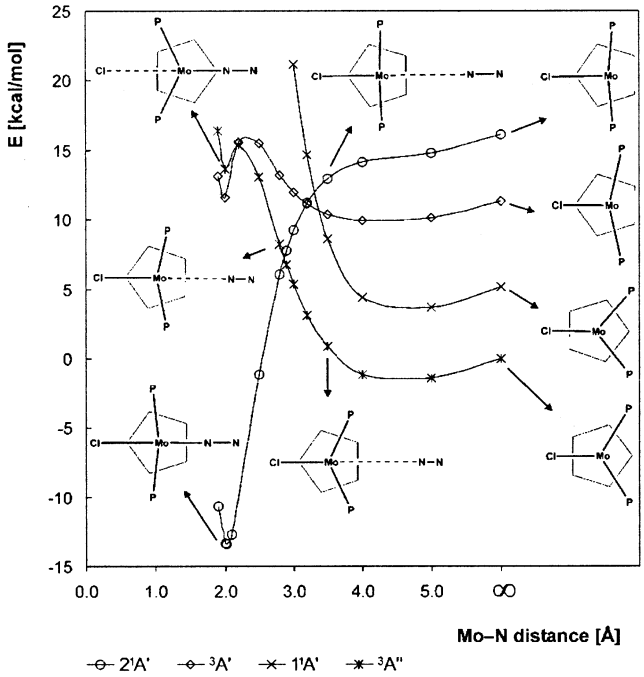


**Figure 1.** B3LYP/DZP LT curves for the coordination of $N_2$ to the four lowest electronic states of $CpMoCl(PH_3)_2$. The states are labeled according to the order in the educt. Key optimized structures are viewed along the Mo−Cp centroid axis. The constrained optimizations were performed within $C_s$ symmetry. We verified, however, that each structure along the LT curves involves the energetically most stable of the two possible $C_s$-symmetric rotational conformations of the Cp ring.

**TABLE 1: Geometry Parameters and Relative Energies of the Educts, $CpMoCl(PH_3)_2$[a]**

| | $^3A''$ | $^3A'$ | $1^1A'$ | $2^1A'$ |
|---|---|---|---|---|
| Mo−Cp(av)[b] | 2.408 | 2.367 | 2.401 | 2.375 |
| Mo−Cl | 2.436 | 2.519 | 2.415 | 2.509 |
| Mo−P | 2.458 | 2.506 | 2.396 | 2.443 |
| Cl−Mo−P | 89.9 | 82.7 | 96.3 | 82.3 |
| P−Mo−P | 92.2 | 115.9 | 82.3 | 103.4 |
| $\Delta E$ (B3LYP/TZD2P)[c] | 0.0 | 11.2 | 5.6 | 16.5 |

[a] Bond distances in angstroms, angles in degrees, and energies in kcal/mol relative to the triplet ground state, $^3A''$. [b] Average Mo−C distance to the cyclopentadienyl ring. [c] SP calculation using the B3LYP/DZP geometry.

opening angles between the different states is perhaps the most striking feature; the two singlet states, for example, differ by more than 20°, P−Mo−P = 82.3° ($1^1A'$) and 103.4° ($2^1A'$). The latter state thus can be characterized as having a geometry suitable for complexation of an additional ligand trans to Cl, and this geometric effect is brought about by a double occupancy of the a″ d orbital. The angular parameters of the previously reported[22] optimized structures of triplet and singlet $CpMoCl(PH_3)_2$ are in excellent agreement with the present angles for $^3A''$ and $1^1A'$. In particular, the reported angle P−Mo−P = 83.8° for the singlet asymptote fragment assumed in the previous study identifies this state as the most stable singlet ($1^1A'$). Thus, the importance of considering more than one singlet state for the addition reaction is immediately evident when comparing with the potential curves in Figure 1. The ground state of the addition product, $CpMoCl(PH_3)_2N_2$, actually is derived from the second lowest singlet state in the educt ($2^1A'$). Moreover, in the educt and at long Mo−N distances, this state is actually the least stable of all the four considered. In the lowest lying singlet state of the educt ($1^1A'$), the potential a′-acceptor orbitals are already occupied resulting in a strongly repulsive potential at Mo−N distances shorter than 4 Å. The singlet potential curves of $N_2$- and CO-addition in the previous study drop in energy below 4 Å, which shows that the correct state ($2^1A'$) was followed in the constrained optimizations. At 4 Å, however, these singlet curves implied several kcal/mol destabilization compared to infinitely separated educts as a result of the comparison to the $1^1A'$ asymptote. The apparent resulting barrier was incorrectly interpreted as being caused by $PH_3-N_2$ repulsive interactions. The present $2^1A'$ potential is attractive already at long distances and describes Mo−N bond formation without a barrier. The other three potentials are also attractive at long distances. The two triplet states may in fact form meta-stable complexes with $N_2$. Since the $16e^-$ triplet complexes are already electronically saturated, the bond formation proceeds in concert with weakening of the other Mo−ligand bonds, in particular Mo−Cl and Mo−C of the Cp ring, and with moderate degree of delocalization of the two unpaired electrons from the metal to the ligands (mainly Cp and $N_2$). The result is an activated addition process. In the case of $N_2$, the activation needed is significant since the Mo−N bond being formed is the weakest of the Mo−ligand bonds in this complex and the process is endothermic. Interestingly, the preferred addition product spin-triplet state is $^3A'$ (and not the ground state of the educt, $^3A''$), which again underlines the importance of monitoring more than one electronic state of each spin multiplicity for the current system. The triplet addition product will be characterized in more detail in the case of CO, for which full optimization of this product of addition to $CpMoCl(PMe_3)_2$ has been performed (vide infra).

In the initial study[22] the barrier associated with $N_2$ addition to $CpMoCl(PH_3)_2$ was approximated by the point of crossing of the spin-triplet and singlet LT curves obtained using the Mo−N distance as the constrained variable. This point (at a distance Mo−N = 2.917 Å) was only ca. 1 kcal/mol higher than that calculated for a triplet complex early in the $N_2$-addition process (Mo−N = 3.917 Å). Minor changes in the computational methodology or in the model complex, e.g., such as increased steric bulk following the use of realistic phosphine groups, thus could reverse the picture and instead predict a barrier due to steric hindrance in the spin-triplet entrance channel. However, our current energy profiles (Figure 1) place the crossing point at significantly higher energies than the first part of the spin-triplet curve and thus strongly support the conclusion that the activation barrier of the addition process is actually controlled by the cost of changing the spin state.[22] In other words, the preferred route seems to be for the system to follow the $^3A''$ state until reaching the region where this PES crosses the $2^1A'$ PES (at a distance Mo−N = 2.8−2.9 Å), undergo spin inversion and follow the latter singlet state to the product. While the lower estimate of the activation energy of $N_2$ addition was taken to be 4.2 kcal/mol on the basis of LT curves in the initial study, our current curves suggest a barrier of 7−8 kcal/mol.

To further characterize this apparent two-state reaction, we have now located the lowest point on the seam of crossing in the region of interest, i.e., the minimum energy crossing point (MECP), as depicted in Figure 2. Relative energies and geometrical parameters for the MECP and the spin-singlet addition product are given in Table 2. The B3LYP/DZP optimized MECP is located at an Mo−N distance of 2.859 Å and has an energy 10.7 kcal/mol higher than that of the triplet educt asymptote. This implies an additional cost of obtaining identical triplet and singlet geometries amounting to 3−4 kcal/mol compared to the point of crossing of the LT curves. As

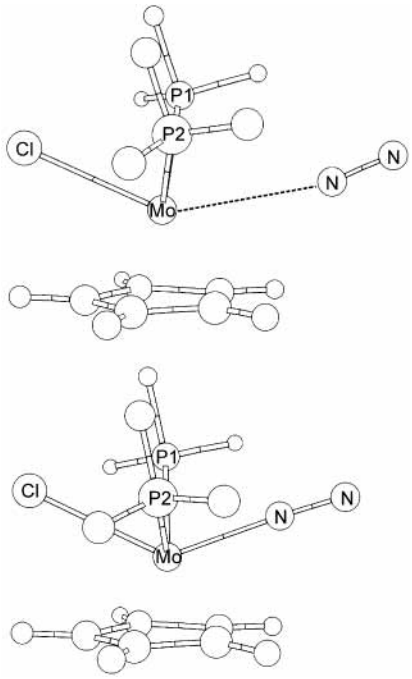


**Figure 2.** B3LYP/DZP optimized structures of the MECP between the $2^1A'$ and $^3A''$ PESs during addition of $N_2$ to $CpMoCl(PH_3)_2$ (uppermost structure) and the spin-singlet product of $N_2$ addition (lower). The latter structure is $C_s$-symmetric whereas the geometry of the MECP displays minor deviations from $C_s$ symmetry.

**TABLE 2: Geometry Parameters and Relative Energies of the MECP and Product of $N_2$ Addition to $CpMoCl(PH_3)_2$[a]**

| | MECP ($^3A/^1A$) | product ($^1A'$) |
|---|---|---|
| Mo−Cp(av)[b] | 2.413 | 2.392 |
| Mo−Cl | 2.501 | 2.583 |
| Mo−P1 | 2.471 | 2.470 |
| Mo−P2 | 2.472 | 2.470 |
| Mo−N | 2.859 | 2.024 |
| Cl−Mo−P1 | 79.5 | 74.0 |
| Cl−Mo−P2 | 79.7 | 74.0 |
| P−Mo−P | 97.8 | 112.8 |
| Cl−Mo−N | 145.8 | 133.7 |
| Mo−N−N | 164.8 | 176.7 |
| Cl−Mo−N−N | −30.8 | 180.0 |
| $\Delta E$ (B3LYP/DZP) | 10.7 | −13.4 |
| $\Delta E$ (B3LYP/TZD2P)[c] | 13.5 | −12.3 |
| $\Delta H_{298}$ (B3LYP/TZD2P)[c] | 13.6 | −10.5 |

[a] Bond distances in angstroms, angles in degrees and energies in kcal/mol relative to separated ground-state educts. [b] Average Mo−C distance to the cyclopentadienyl ring. [c] SP calculation using the B3LYP/DZP geometry. The average of the singlet and triplet energies is used for the MECP ($\Delta\Delta E = |\Delta E_{triplet} - \Delta E_{singlet}| \leq 0.3$).

expected the MECP is seen to have a geometry intermediate between the partially optimized singlet and triplet geometries in this region. The P−Mo−P angle for example, is 94.0° in the triplet and 105.8° in the singlet complex at a distance Mo−N = 2.9 Å and 97.8° in the MECP. At the MECP geometry the B3LYP/DZP description apparently involves a nonnegligible basis set superposition error (BSSE), and our single-point (SP) energy calculations with larger basis sets shift the barrier upward by 3 kcal/mol, resulting in a final estimate ($\Delta E^{\ddagger} = 13.5$ kcal/mol) in excellent agreement with the experimental result for $Cp^*MoCl(PMe_3)_2$ ($\Delta E^{\ddagger} = 14.5$ kcal/mol).[22] The calculated exothermicity, however, is more than 12 kcal/mol lower than that experimentally determined for $Cp^*MoCl(PMe_3)_2$ and this discrepancy will be examined in the section below concerning

**TABLE 3: Energies of Excited States of $CpMoCl(PH_3)_2$ Given Relative to the Triplet Ground State, $^3A''$[a]**

| | $^3A'$ | $1^1A'$ | $2^1A'$ |
|---|---|---|---|
| B3LYP/DZP | 11.3 | 5.2 | 16.1 |
| B3LYP/TZD2P[b] | 11.2 | 5.6 | 16.5 |
| BPW91/TZD2P[b] | 10.9 | 2.9 | 14.5 |
| RHF/TZD2P[b] | 11.1 | 19.5 | 26.9 |
| CASSCF/TZD2P[b] | 11.1 | 16.2 | 20.5 |
| MRMP2/TZD2P[b] | 11.2 | 7.1 | 24.3 |

[a] Electronic energies given in kcal/mol. [b] SP calculation using the B3LYP/DZP geometry.

$N_2$ addition to $CpMoCl(PMe_3)_2$. The first section below deals with the (technical) validation of the quantum chemical description of the four low-lying electronic states of the educt. The chemically oriented reader may skip this section altogether.

**Stability of the Spin States: Validation of the Computational Approach.** Because of the involvement of more than one spin state in the current reactions, it is of vital importance that these states are described with sufficiently even accuracy by the methods with which they are studied. Unfortunately, experimental excitation energies for the $16e^-$ educts, $CpMoCl(PR_3)_2$, are not known and comparison has to be made against computational results from higher level methods. The computationally more tractable model, $CpMoCl(PH_3)_2$, was chosen for the validation studies using a multiconfigurational second-order perturbational method, MRMP2, in combination with basis sets essentially of the type triple-$\zeta$ plus diffuse functions and double polarization (termed TZD2P, see the Computational Details section). The reference CASSCF wave functions involved an active space of four electrons (the d electrons) and three orbitals, which should take into account the most important part of the static correlation expected in particular for the singlet states. This expectation is confirmed by the fact that the CASSCF wave function was found to be an equally good reference function in the four states studied for the $16e^-$ reactant, with the reference weight calculated to be 65% in all cases.

Turning now to the lowest lying singlet state ($1^1A'$), its stability is seen to be highly dependent on the correlation treatment (see Table 3), with the nonvertical excitation energy from the triplet ground state ($^3A''$) being reduced from 15−20 kcal/mol calculated using HF and CASSCF to ca. 7 kcal/mol upon inclusion of dynamical correlation in the form of second-order perturbation theory. The earlier single-reference MP2 calculations,[22] which did not involve polarization (correlating) functions, gave 10.9 kcal/mol for this excitation. Improving the correlation treatment and the basis sets compared to the present case is likely to stabilize this singlet even further. The true value for the singlet−triplet gap is probably somewhat lower than 7 kcal/mol, and thus in good accord with the DFT results (2.9 and 5.6 kcal/mol for BPW91 and B3LYP, respectively). The two other excitation energies are considerably less dependent on the correlation treatment. For the second triplet ($^3A'$) which also has the same requirements as the ground state with respect to exchange, the different methods give virtually identical results. The second singlet state ($2^1A'$) has the two d electron pairs in orbitals belonging to different irreducible representations and its stability is much less dependent on the correlation treatment than that of the most stable singlet. MRMP2 predicts an energy difference from the triplet ground state within 3 kcal/mol from that of Hartree−Fock. We can thus conclude that the ab initio result probably is close to converged and that the DFT methods overestimate the stability of this state somewhat due to inadequacies in the exchange part of the functionals. The hybrid functional, B3LYP, includes some exact (HF) exchange

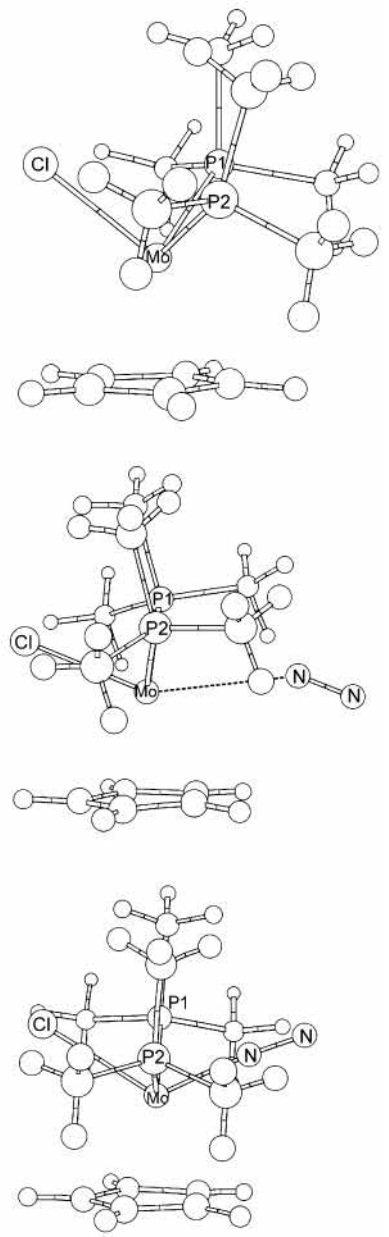


**Figure 3.** B3LYP/DZP optimized structures of the triplet educt (upper structure), MECP (middle) and spin-singlet product (lower) of $N_2$ addition to $CpMoCl(PMe_3)_2$. The two latter structures are $C_s$-symmetric, whereas the geometry of the educt deviates slightly from $C_s$ symmetry.

and is 2 kcal/mol closer to the MRMP2 result than the pure density functional, BPW91.

**Addition of $N_2$ to $CpMoCl(PMe_3)_2$.** Addition of $N_2$ to $CpMoCl(PMe_3)_2$ is assumed to proceed in a fashion similar to that described above for $CpMoCl(PH_3)_2$. Thus, for the more realistic $PMe_3$ analogue only the ground-state triplet reactant, the singlet product and the MECP have been subjected to calculation in order to investigate the influence of the phosphine methyl groups. In other words, at any given point we only calculated the lowest state for each spin multiplicity which furthermore allowed us to explore the potential surfaces without symmetry restrictions. The three optimized geometries are shown in Figure 3, with accompanying geometrical parameters and relative energies in Table 4. Only the educt, $CpMoCl(PMe_3)_2$, is seen to depart from $C_s$ symmetry. The two trimethyl phosphine groups are rotated slightly away from an eclipsed conformation in order to reduce steric repulsion, resulting in a 1° difference between the two Cl−Mo−P angles. A similar but much more pronounced departure from symmetry is evident in the crystal structure of Cp*MoCl(dppe).[38] This difference between experiment and theory can be explained by the presence of the $C_2H_4$ bridge and the sterically more demanding Cp* ligand in the experimentally determined structure. Both these features contribute to a sharper P−Mo−P angle compared to our calculations on the Cp containing model, the difference amounting to 20°. The sharper P−Mo−P angle, in turn, obviously increases the steric repulsion between the trimethyl phosphine groups resulting in a larger rotation away from the eclipsed conformation. Apart from the deviation in P−Mo−P angle already commented upon, the calculated geometrical parameters are in good accord with those available from related, experimentally determined structures, with the possible exception of the Mo−N and Mo−Cl distances of the singlet product, which are calculated to be too short and too long, respectively (see Table 4). A detailed comparison of these theoretically and experimentally obtained distances is perhaps not justified, however, since N/Cl disorder has been noted in the refinement of the X-ray structures.[39] A similar deviation (and possible explanation) was observed also for the MP2-optimized singlet product in the initial study.[22] Finally, the located MECP is $C_s$ symmetric but otherwise very similar to the MECP presented for the $PH_3$ analogue above. This confirms our assumption that the general features of the $N_2$-addition process should remain when going from $PH_3$ to $PMe_3$.

Perhaps somewhat surprising is the fact that the spin-inversion-related barrier to $N_2$ addition remains practically identical when replacing $PH_3$ by $PMe_3$, demonstrating the minor influence of steric effects on the barrier height. Changing the DFT functional apparently also results in only minor difference in the calculated barrier height. The stability of the calculated activation enthalpy with respect to variation of both the model complexes and the method of calculation suggests that it is not only fortuitous that our best estimates are in excellent agreement with the measurements for $Cp^*MoCl(PMe_3)_2$.[22] This further serves to underline that the rate of this addition reaction is indeed controlled by the spin-inversion process and that the MECP appears to be a good approximation to the adiabatic transition state formed by the avoided crossing and may provide useful estimates of the activation energies for spin flips.[2−4] For the title compounds it was not deemed practical to perform accurate calculation of the spin−orbit coupling, and thus the transmission coefficient with which our enthalpic barrier is associated remains unknown. The fair agreement between the calculated and experimental entropic terms (Table 4), however, suggests that the spin−orbit coupling is large, as often found for compounds of second-row transition metals.[1−4]

As mentioned above for the $PH_3$ analogue, the exothermicity of the $N_2$-addition process is less straightforward to predict. For the $PH_3$ analogue, we calculated an exothermicity more than 12 kcal/mol lower than that experimentally recorded for $Cp^*MoCl(PMe_3)_2$. The realistic phosphine groups improves the estimate by 2−3 kcal/mol (Table 4) and most of the remaining error of almost 10 kcal/mol can probably be attributed to inadequacies in the B3LYP functional, most likely due to the correlation part. The pure density functional (BPW91) estimate is within the error bars of the experiment for the reaction (−22.8 ± 2.1 kcal/mol) as well as the activation enthalpy (14.0 ± 1.0 kcal/mol).

**Addition of CO to $CpMoCl(PMe_3)_2$.** Stabilization compared to separated reagents was noted at long Mo−N distances for the calculated potential curves of $N_2$ addition above. A similar stabilization for CO would imply that the highest point on the

**TABLE 4: Geometry Parameters and Relative Energies of the Triplet Educt, MECP, and Singlet Product of $N_2$ Addition to $CpMoCl(PMe_3)_2$[a]**

| | educt ($^3A$) | | MECP ($^3A''/^1A'$) | | product ($^1A'$) | |
|---|---|---|---|---|---|---|
| | calcd | exptl[b] | calcd | exptl[c] | calcd | exptl[d] |
| Mo−Cp(av)[e] | 2.425 | 2.335(4) | 2.425 | | 2.403 | 2.328 |
| Mo−Cl | 2.464 | 2.416(1) | 2.530 | | 2.611 | 2.527 |
| Mo−P1 | 2.476 | 2.428(1) | 2.496 | | 2.518 | 2.464 |
| Mo−P2 | 2.467 | 2.413(1) | 2.496 | | 2.518 | 2.464 |
| Mo−N | | | 2.910 | | 1.978 | 2.158 |
| Cl−Mo−P1 | 89.2 | 83.59(4) | 81.0 | | 76.1 | 77.33 |
| Cl−Mo−P2 | 90.1 | 92.94(5) | 81.0 | | 76.1 | 77.33 |
| P−Mo−P | 98.4 | 78.71(4) | 103.9 | | 126.1 | 114.4 |
| Cl−Mo−N | | | 151.1 | | 123.3 | 131.5 |
| Mo−N−N | | | 152.8 | | 175.9 | |
| Cl−Mo−N−N | | | 180.0 | | 180.0 | |
| $\Delta E$ (B3LYP/DZP) | 0.0 | 0.0 | 11.8 | $14.0 \pm 1.0$ | −16.6 | $-22.8 \pm 2.1$ |
| $\Delta E$ (B3LYP/TZD2P)[f] | 0.0 | 0.0 | 14.2 | $14.0 \pm 1.0$ | −15.8 | $-22.8 \pm 2.1$ |
| $\Delta H$ (B3LYP/TZD2P)[f] | 0.0 | 0.0 | 14.3 | $14.0 \pm 1.0$ | −13.3 | $-22.8 \pm 2.1$ |
| $\Delta H$ (BPW91/TZD2P)[f] | 0.0 | 0.0 | 14.4 | $14.0 \pm 1.0$ | −21.2 | $-22.8 \pm 2.1$ |
| $\Delta S$ (B3LYP/DZP) | 0 | 0 | −29 | $-20 \pm 3$ | −38 | $-67 \pm 7$ |

[a] Bond distances in angstroms, angles in degrees, energies/enthalpies in kcal/mol and entropies in cal/(mol·K). Energy data given relative to separated ground-state educts. [b] Geometry parameters from X-ray crystal structure of Cp*MoCl(dppe).[38] [c] Activation parameters for $N_2$ addition to $Cp^*MoCl(PMe_3)_2$.[22] [d] Structural parameters calculated from fractional coordinates published for $Cp^*MoCl(PMe_3)_2(N_2)$.[39] Reaction energetics measured for $N_2$ addition to $Cp^*MoCl(PMe_3)_2$.[22] [e] Average Mo−C distance to the cyclopentadienyl ring. [f] SP calculation using the B3LYP/DZP geometry. The average of the singlet and triplet energies is used for the MECP ($\Delta\Delta E = |\Delta E_{triplet} - \Delta E_{singlet}| \leq 1.3$).

potential curve of coordination for the triplet state should not be located at long Mo−CO distances as found in the initial study,[22] and it would require detailed theoretical investigation to judge whether the recorded activation enthalpy (5.0 kcal/mol for addition to the Cp* analogue) is due simply to a barrier to addition on the triplet PES or to the spin inversion process. Accordingly, we have calculated the LT potential curve of CO addition to the lowest lying spin-triplet state ($1^3A$) and the second lowest singlet state ($2^1A$) of $CpMoCl(PMe_3)_2$. For $2^1A$, only the section of the reaction coordinate for which this state can be expected to be the lowest lying of singlet multiplicity (Mo−CO distance shorter than 3 Å) has been calculated in order to avoid using symmetry restrictions (vide supra). The two resulting potential curves are shown in Figure 4. Indeed, a barrier to CO addition on the triplet PES analogous to that calculated for $N_2$ (Figure 1) is evident. This time, however, the bond being formed (Mo−CO) is stronger than those being weakened (Mo−Cl and Mo−C of the Cp ring), and hence the triplet state bond formation for CO is found to occur earlier, and to require less activation than addition of $N_2$ (Figure 1). The origin of the barrier, rehybridization associated with simultaneous bond rupture and formation, however, remains the same in the two cases. The maximum on the LT curve is located close to a Mo−CO distance of 2.6 Å, whereas the two LT curves cross at a longer Mo−CO distance (2.9 Å) and at an energy ca. 1.5 kcal/mol lower than the maximum on the triplet curve. The latter result may suggest that the spin inversion takes place before reaching the classical barrier on the triplet PES, i.e., that the reaction is qualitatively similar to that of $N_2$. However, the difference in energy between the point of crossing of the two LT curves and the maximum on the triplet curve is tiny and a more detailed comparison between the triplet state barrier and the crossing region is required before drawing any conclusions regarding the nature of the barrier.

To this end, we have performed full optimization of the transition state (TS) of CO addition on the triplet PES as well as of two different MECPs between the two spin states, as shown in Figure 5 and with accompanying geometrical parameters and relative energies given in Table 5. The TS has a distance Mo−CO = 2.573 Å and is structurally and energetically similar to

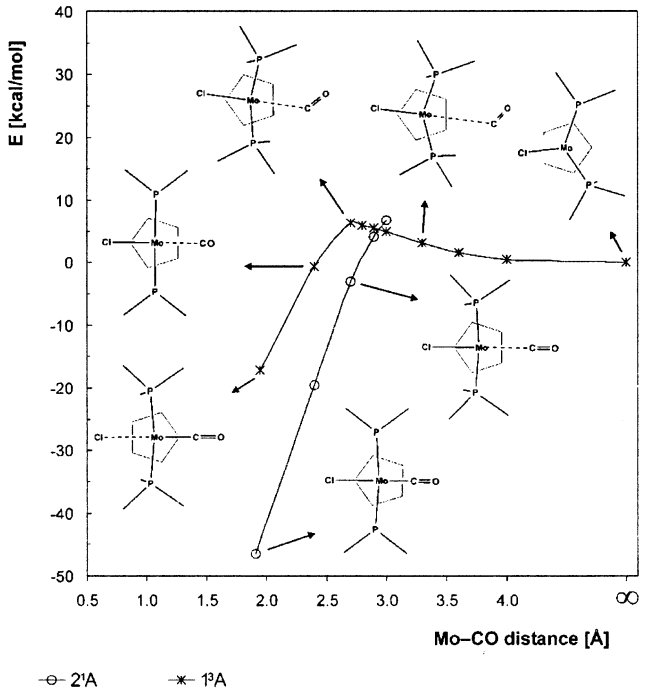


**Figure 4.** B3LYP/DZP LT curves for the coordination of CO to the lowest triplet state ($1^3A$) and the second lowest doublet state ($2^1A$) of $CpMoCl(PMe_3)_2$. The states are labeled according to the order in the educt assuming $C_1$ symmetry. Key optimized structures are viewed along the Mo−Cp centroid axis. The LT constrained optimizations were performed without symmetry restrictions. The points pertaining to the spin-triplet educt (infinite Mo−CO distance) as well as the two addition products (the two leftmost points) involve full, unconstrained optimizations.

the LT maximum in Figure 4. The imaginary frequency (100i $cm^{-1}$) corresponds to a virtually pure Mo−CO stretching mode as expected. The optimized crossing points are both of shorter Mo−CO bonds and lower energies and must be characterized as being located after the spin-triplet TS on the reaction coordinate. No MECP could be located at distances comparable to or longer than that of the triplet TS. The first MECP (MECP1, Mo−CO = 2.332 Å) is located between the TS and the product

**TABLE 5: Geometry Parameters and Relative Energies of Stationary Points and MECPs of CO Addition to $CpMoCl(PMe_3)_2$[a]**

| | TS ($^3$A) | | MECP1[b] ($^3$A/$^1$A) | MECP2[b] ($^3$A/$^1$A) | product ($^3$A′) | product ($^1$A′) | |
|---|---|---|---|---|---|---|---|
| | calcd | exptl[c] | calcd | calcd | calcd | calcd | exptl[d] |
| Mo−Cp(av)[e] | 2.437 | | 2.405 | 2.601 | 2.580 | 2.422 | 2.335(9) |
| Mo−Cl | 2.509 | | 2.540 | 2.719 | 2.743 | 2.617 | 2.577(5) |
| Mo−P1 | 2.532 | | 2.547 | 2.521 | 2.522 | 2.509 | 2.469(2) |
| Mo−P2 | 2.522 | | 2.549 | 2.523 | 2.522 | 2.509 | 2.479(2) |
| Mo−CO | 2.573 | | 2.332 | 1.948 | 1.946 | 1.913 | 1.874(11) |
| Cl−Mo−P1 | 79.9 | | 79.6 | 78.2 | 77.6 | 75.9 | 76.5(1) |
| Cl−Mo−P2 | 85.0 | | 79.5 | 78.1 | 77.6 | 75.9 | 79.7(1) |
| P−Mo−P | 101.4 | | 128.4 | 118.0 | 117.1 | 128.1 | 116.6(1) |
| Cl−Mo−CO | 146.7 | | 123.7 | 154.3 | 153.0 | 119.1 | 130.2(4) |
| Mo−C−O | 124.3 | | 119.3 | 176.2 | 177.1 | 177.5 | |
| Cl−Mo−C−O | −129.9 | | −179.3 | 1.4 | 0.0 | 180.0 | |
| $\Delta E$ (B3LYP/DZP) | 6.5 | 5.0 ± 0.3 | 1.2 | −17.2 | −17.2 | −46.6 | |
| $\Delta E$ (B3LYP/TZD2P)[f] | 8.6 | 5.0 ± 0.3 | 3.3 | −12.7 | −13.7 | −43.7 | |
| $\Delta H$ (B3LYP/TZD2P)[f] | 9.9 | 5.0 ± 0.3 | 4.0 | −11.4 | −11.4 | −40.8 | |
| $\Delta H$ (BPW91/TZD2P)[f] | 6.7 | 5.0 ± 0.3 | −2.8 | −18.3 | −17.1 | −50.4 | |
| $\Delta S$ (B3LYP/DZP) | −34 | −35 ± 4 | −32 | −34 | −30 | −41 | |

[a] Bond distances in angstroms, angles in degrees, energies/enthalpies in kcal/mol and entropies in cal/(mol·K). Energy data given relative to separated ground-state educts. [b] The first and second MECP located on the reaction coordinate, respectively, as judged from the Mo−CO distances. [c] Activation parameters for CO addition to $Cp^*MoCl(PMe_3)_2$.[22] [d] X-ray crystal structure of $Cp^*MoCl(PMe_2Ph)_2(CO)$.[38] [e] Average Mo−C distance to the cyclopentadienyl ring. [f] SP calculation using the B3LYP/DZP geometry. For the MECPs, the average of the singlet and triplet energies is used ($\Delta\Delta E = |\Delta E_{triplet} - \Delta E_{singlet}| \leq 2.4$).

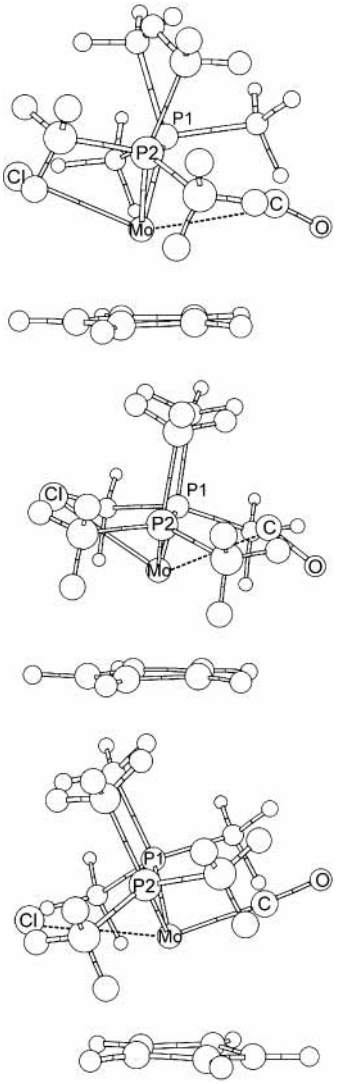


**Figure 5.** B3LYP/DZP optimized structures of the transition state (TS) of CO addition to $CpMoCl(PMe_3)_2$ on the lowest spin-triplet PES (uppermost structure, $C_1$ symmetric, $^3$A) as well as the first (middle, $^3$A/$^1$A) and second (lower, $^3$A/$^1$A) located MECP. The two MECPs are close to $C_s$ symmetric.

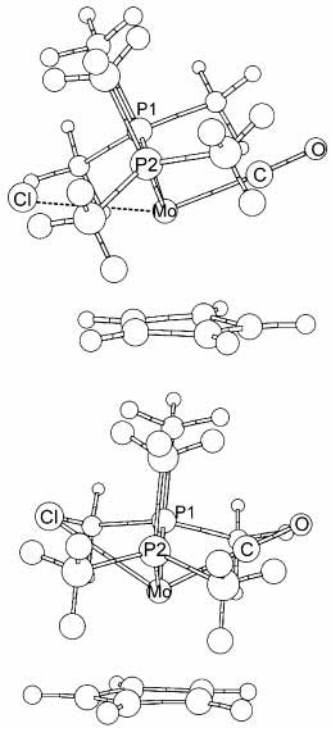


**Figure 6.** B3LYP/DZP optimized structures of the spin-triplet (uppermost structure, $^3$A′) and singlet (lower, $^1$A′) product of CO addition to $CpMoCl(PMe_3)_2$.

of addition, while MECP2 is structurally and energetically close to the product located on the diabatic spin-triplet PES (see Figure 6). According to these results the reaction proceeds by coordination on the spin-triplet PES and the system is likely to remain a spin triplet until reaching the classical TS. After the TS the system may undergo spin inversion en route to (MECP1) or at the triplet product (MECP2), with the latter alternative being the more likely. In other words, the barrier of the CO-addition reaction is expected to be identical to that calculated for addition on the diabatic-triplet PES and not to be due to the spin inversion process. This contrast to the $N_2$ addition is brought about by the difference in stability of the triplet product. Spin-triplet minima were located also for the $N_2$-addition product (Figure

1), but these were found to be unstable with respect to the triplet educt asymptote by more than 10 kcal/mol and to be accompanied by significant activation barriers. As noted in the initial study,[22] the formation of the triplet product is exothermic for CO because CO is the better ligand. $N_2$ on the other hand, is the weakest of all the ligands in the title complexes and the formation of a Mo−$N_2$ complex at the expense of weakening the bonds to the other ligands is disfavored. Comparison of the bond distances of the spin-triplet addition product, $CpMoCl(PMe_3)_2(CO)$ (Table 5), with those of the corresponding educt (Table 4) shows that the result of the addition of CO on the triplet PES is a 0.28 Å lengthening of the Mo−Cl bond and an increase of the average Mo−C distance of the Cp ring by 0.15 Å, whereas the Mo−P bond lengths are affected by only 0.05−0.06 Å. The increase in the average distance to the Cp carbon atoms reflects a reduction in hapticity of the Mo−Cp bond. Whereas in the reactant, all these Mo−C distances are in the range 2.387−2.470 Å, the cyclopentadienyl anion is unsymmetrically bonded in the triplet product, with corresponding distances 2.438−2.782 Å. These bond weakenings are also reflected in the fact that the two unpaired electrons, which are almost exclusively attributed to the metal in the triplet reactant (Mulliken spin density 1.91 *e*), are partly delocalized on the ligands in the triplet product, with a Mulliken spin density reduced to 1.56 *e* for the metal. Most of this difference in spin density is taken over by the cyclopentadienyl, in particular by the carbon atom with the longest Mo−C distance, and by CO. For the $N_2$-addition process, the BPW91/TZD2P calculated relative energies were seen to be in excellent agreement with experimental results for both the activation barrier and the overall reaction enthalpy (Table 4). Also for CO the agreement between the experimental and BPW91/TZD2P calculated activation enthalpy is convincing (within 2 kcal/mol, Table 5). The experimental CO-addition reaction enthalpy is not available, but our calculations suggest a $\Delta H_{298}$ close to −50 kcal/mol.

The calculated singlet product structure is in good accord with the X-ray crystal structure of $Cp^*MoCl(PMe_2Ph)_2(CO)$,[38] although with a somewhat too wide P−Mo−P angle as also noted for the $N_2$-addition product (vide supra). The state of the spin-triplet addition product ($^3A'$) is identical to that found as the most stable for triplet $CpMoCl(PH_3)_2(N_2)$ (vide supra). Also the nearly $C_s$-symmetric MECPs display an orbital occupancy for the triplet state commensurate with $^3A'$.

## Conclusions

We have studied the addition of the ligands $N_2$ and CO to the complexes $CpMoCl(PR_3)_2$ (R = H and Me) using DFT. It has been found necessary to include more than one electronic state of each spin multiplicity (triplet and singlet) to arrive at a qualitatively correct description of these addition reactions: The ground state of the $18e^-$ addition products is actually derived from the second lowest singlet state of the $16e^-$ educts (term symbol $2^1A'$ in case of a $C_s$-symmetric complex), whereas the preferred state of the spin-triplet addition products is derived from the second lowest triplet state of the $16e^-$ educt ($^3A'$).

The current calculations firmly place the barrier of addition at Mo−ligand distances below 3 Å where the bond-breaking and -forming on the spin-triplet PES is already well under way. Steric hindrance at long Mo−ligand distances, on the other hand, is found to be of little importance. The $2^1A'$ state drops in energy throughout addition and the accompanying LT curve crosses the curve for the $^3A''$ state at a Mo−ligand distance slightly below 3 Å (2.8−2.9 Å) for both of the ligands $N_2$ and CO. For $N_2$, the TS of the endothermic addition on the triplet PES is located much later on the reaction coordinate (at a distance Mo−N ≈ 2.2 Å for R = H) and at significantly higher energies, thus making spin inversion before reaching this TS the preferred alternative. For CO on the other hand, the TS of the exothermic addition on the triplet PES is located only shortly after and at slightly higher energies than the point of crossing of the two LT curves and the balance between a classical barrier as caused by the TS and a spin-inversion related barrier turns out to be of a more delicate nature. Our current computational approach is in favor of the former alternative, thus indicating that the preferred route of CO addition is for the system to remain a spin triplet until after the TS. Finally, our mechanistic findings are supported by excellent agreement between the calculated activation and reaction enthalpies and those experimentally available for addition of $N_2$ and CO to $Cp^*MoCl(PMe_3)_2$.

**Acknowledgment.** We thank the Conseil Régional de Bourgogne for funding to upgrade our computing facility and CINES for a grant of CPU time. V.R.J. thanks the CNRS for a research fellowship. We also thank Jeremy N. Harvey for providing us with his MECP location program and for helpful discussions.

## References and Notes

(1) Schröder, D.; Shaik, S.; Schwarz, H. *Acc. Chem. Res.* **2000**, *33*, 139.
(2) Harvey, J. N. In *Computational Organometallic Chemistry*; Cundari, T. R., Ed.; Marcel Dekker: New York, 2001.
(3) Harvey, J. N.; Poli, R.; Smith, K. M. *Coord. Chem. Rev.* In press.
(4) Poli, R.; Harvey, J. N. *Chem. Soc. Rev.* **2003**, *32*, 1.
(5) Poli, R. *Acc. Chem. Res.* **1997**, *30*, 494.
(6) Shaik, S.; Danovich, D.; Fiedler, A.; Schröder, D.; Schwarz, H. *Helv. Chim. Acta* **1995**, *78*, 1393.
(7) Musaev, D. G.; Morokuma, K. *J. Phys. Chem.* **1996**, *100*, 11600.
(8) Harris, N.; Shaik, S.; Schröder, D.; Schwarz, H. *Helv. Chim. Acta* **1999**, *82*, 1784.
(9) Porembski, M.; Weisshaar, J. C. *J. Phys. Chem. A* **2001**, *105*, 4851.
(10) Shaik, S.; Filatov, M.; Schröder, D.; Schwarz, H. *Chem. Eur. J.* **1998**, *4*, 193.
(11) Filatov, M.; Harris, N.; Shaik, S. *Angew. Chem., Int. Ed. Engl.* **1999**, *38*, 3510.
(12) Jin, N.; Groves, J. T. *J. Am. Chem. Soc.* **1999**, *121*, 2923.
(13) Harvey, J. N. *J. Am. Chem. Soc.* **2000**, *122*, 12401.
(14) Smith, K. M.; Poli, R.; Harvey, J. N. *Chem. Eur. J.* **2001**, *7*, 1679.
(15) Green, J. C.; Harvey, J. N.; Poli, R. *J. Chem. Soc, Dalton Trans.* **2002**, 1861.
(16) Deng, L. Q.; Margl, P.; Ziegler, T. *J. Am. Chem. Soc.* **1999**, *121*, 6479.
(17) Deng, L. Q.; Schmid, R.; Ziegler, T. *Organometallics* **2000**, *19*, 3069.
(18) Khoroshun, D. V.; Musaev, D. G.; Vreven, T.; Morokuma, K. *Organometallics* **2001**, *20*, 2007.
(19) Döhring, A.; Jensen, V. R.; Jolly, P. W.; Thiel, W.; Weber, J. C. *Organometallics* **2001**, *20*, 2234.
(20) Jensen, V. R.; Thiel, W. *Organometallics* **2001**, *20*, 4852.
(21) Poli, R. *Chem. Rev.* **1996**, *96*, 2135.
(22) Keogh, D. W.; Poli, R. *J. Am. Chem. Soc.* **1997**, *119*, 2516.
(23) Abu-Hasanayn, F.; Cheong, P.; Oliff, M. *Angew. Chem., Int. Ed. Engl.* **2002**, *41*, 2120.
(24) Becke, A. D. *J. Chem. Phys.* **1993**, *98*, 5648.
(25) Frisch, M. J.; Trucks, G. W.; Schlegel, H. B.; Scuseria, G. E.; Robb, M. A.; Cheeseman, J. R.; Zakrzewski, V. G.; Montgomery, J. A., Jr.; Stratmann, R. E.; Burant, J. C.; Dapprich, S.; Millam, J. M.; Daniels, A. D.; Kudin, K. N.; Strain, M. C.; Farkas, O.; Tomasi, J.; Barone, V.; Cossi, M.; Cammi, R.; Mennucci, B.; Pomelli, C.; Adamo, C.; Clifford, S.; Ochterski, J.; Petersson, G. A.; Ayala, P. Y.; Cui, Q.; Morokuma, K.; Malick, D. K.; Rabuck, A. D.; Raghavachari, K.; Foresman, J. B.; Cioslowski, J.; Ortiz, J. V.; Stefanov, B. B.; Liu, G.; Liashenko, A.; Piskorz, P.; Komaromi, I.; Gomperts, R.; Martin, R. L.; Fox, D. J.; Keith, T.; Al-Laham, M. A.; Peng, C. Y.; Nanayakkara, A.; Gonzalez, C.; Challacombe, M.; Gill, P. M. W.; Johnson, B.; Chen, W.; Wong, M. W.; Andres, J. L.; Head-Gordon, M.; Replogle, E. S.; Pople, J. A. *Gaussian 98*, revision A.7; Gaussian, Inc.: Pittsburgh, PA, 1998.
(26) Harvey, J. N.; Aschi, M.; Schwarz, H.; Koch, W. *Theor. Chem. Acc.* **1998**, *99*, 95.

(27) Koga, N.; Morokuma, K. *Chem. Phys. Lett.* **1985**, *119*, 371.
(28) Vosko, S. H.; Wilk, L.; Nusair, M. *Can. J. Phys.* **1980**, *58*, 1200.
(29) Becke, A. D. *Phys. Rev. A* **1988**, *38*, 3098.
(30) Perdew, J. P.; Wang, Y. *Phys. Rev. B* **1992**, *45*, 13244.
(31) Nakano, H. *J. Chem. Phys.* **1993**, *99*, 7983.
(32) Nakano, H. *Chem. Phys. Lett.* **1993**, *207*, 372.
(33) Schmidt, M. W.; Baldridge, K. K.; Boatz, J. A.; Elbert, S. T.; Gordon, M. S.; Jensen, J. H.; Koseki, S.; Matsunaga, N.; Nguyen, K. A.; Su, S. J.; Windus, T. L.; Dupuis, M.; Montgomery, J. A. *J. Comput. Chem.* **1993**, *14*, 1347.
(34) Hay, P. J.; Wadt, W. R. *J. Chem. Phys.* **1985**, *82*, 284.
(35) Hay, P. J.; Wadt, W. R. *J. Chem. Phys.* **1985**, *82*, 299.
(36) Check, C. E.; Faust, T. O.; Bailey, J. M.; Wright, B. J.; Gilbert, T. M.; Sunderlin, L. S. *J. Phys. Chem. A* **2001**, *105*, 8111.
(37) Dunning, T. H.; Hay, P. J. In *Methods of Electronic Structure Theory*; Schaefer, H. F., Ed.; Plenum Press: New York, 1977; p 1.
(38) Abugideiri, F.; Fettinger, J. C.; Keogh, D. W.; Poli, R. *Organometallics* **1996**, *15*, 4407.
(39) Baker, R. T.; Morton, J. R.; Preston, K. F.; Williams, A. J.; Le Page, Y. *Inorg. Chem.* **1991**, *30*, 113.